Biochemical and Biophysical Research Communications 457 (2015) 12–18

Contents lists available at ScienceDirect

Biochemical and Biophysical Research Communications

journal homepage: www.elsevier.com/locate/ybbrc

IRAP deficiency attenuates diet-induced obesity in mice through increased energy expenditure

Manabu Niwa [a], Yasushi Numaguchi [a,*], Masakazu Ishii [a,1], Tomomi Kuwahata [a], Megumi Kondo [a], Rei Shibata [a], Keishi Miyata [b], Yuichi Oike [b], Toyoaki Murohara [a]

[a] Department of Cardiology, Nagoya University Graduate School of Medicine, Nagoya, Japan
[b] Department of Molecular Genetics, Kumamoto University Graduate School of Medicine, Kumamoto, Japan

ARTICLE INFO

Article history:
Received 9 December 2014
Available online 19 December 2014

Keywords:
Brown adipose tissue
Diet-induced obesity
Insulin-regulated aminopeptidase
UCP-1

ABSTRACT

Activation of the adipose renin–angiotensin system contributes to the development of obesity and metabolic syndrome. Insulin-regulated aminopeptidase (IRAP) has been identified a key regulator of GLUT4 transporter as well as angiotensin IV (AngIV) receptor (AT4R). Although AngII-AT1R axis appears as anorexigenic and as an effector of energy expenditure, the impact of AngIV-IRAP/AT4R axis on energy metabolism remains unknown. The aim was to determine the role of IRAP in energy metabolism in mice.

Methods and results: In adipocyte culture, plasminogen activator inhibitor type 1 (PAI-1) expression levels were diminished in IRAP knockout ($IRAP^{-/-}$) if compared with those of wild-type (C57Bl/6J, WT) mice. Mice were fed high-fat diet (32% fat) at age of 8 weeks. At the entry, body weight, body fat content, and parameters of saccharometabolism were similar between groups. However, $IRAP^{-/-}$ mice exhibited blunted body weight gain compared to that of WT mice, despite comparable food intake and physical activity. At 20 weeks of age, $IRAP^{-/-}$ mice had 25% lower body weight than WT mice. Glucose and insulin tolerance tests revealed that the glucose disposal and the hypoglycemic effect of insulin were pronounced in $IRAP^{-/-}$ mice after a high fat diet. Indirect calorimetry demonstrated that whole-body oxygen consumption rates were significantly higher in $IRAP^{-/-}$ mice by 18% with mild hyperthermia. Analysis of brown adipose tissue (BAT) in $IRAP^{-/-}$ showed increased levels of uncoupling protein-1 (UCP-1) at basal level and adaptive thermogenesis was not impaired.

Conclusions: IRAP deficiency may lead to suppression of PAI-1 expression in adipocytes and upregulation of UCP-1-mediated thermogenesis in BAT and increased energy expenditure to prevent the development of obesity, and these facts suggest a therapeutic potential of IRAP/AT4R blockade in diet-induced obesity.

1. Introduction

The activation of adipose renin–angiotensin system (RAS) contributes to the development of obesity and metabolic syndrome subsequent to diabetes and atherosclerosis [1–3]. The main effector peptide of the RAS, angiotensin II (AngII), exerts many actions through the activation of downstream signals by binding to its receptors, namely, angiotensin type 1 and type 2 receptors (AT1R and AT2R, respectively) [4]. Regarding AT1R and obesity, there is increasing evidence that AT1R blockade may contribute to the reduction of obesity in diabetic patients [1–3]. Although AngII-AT1R axis appears as anorexigenic and as an effector of energy expenditure in mice, the exact mechanism by which AngII-AT1R signaling affects on feeding behavior and energy expenditure are complicated and remains unknown [5,6].

Insulin-regulated aminopeptidase (IRAP), also known as AngIV receptor (AT4R), was first identified as a major protein in intracellular vesicles isolated from low-density microsomes of rat fat and muscle cells that also colocalized with the insulin-responsive glucose transporter isotype GLUT4 [7–9]. Based on the facts that IRAP regulates the GLUT4 trafficking in the adipocytes [7–9], we set out to investigate the effects of chronic energy surplus on metabolic

Abbreviations: Ang, angiotensin; AT1R, angiotensin II type 1 receptor; AT2R, angiotensin II type 2 receptor; AT4R, angiotensin IV receptor; BAT, brown adipose tissue; IRAP, insulin-regulated aminopeptidase; PAI-1, plasminogen activator inhibitor type 1; PGC, peroxisome proliferator-activated receptor-γ coactivator; PPAR, peroxisome proliferator-activated receptor; RAS, renin–angiotensin system; UCP, uncoupling protein; WAT, white adipose tissue; WT, wild type.

* Corresponding author at: Department of Cardiology, Nagoya University Graduate School of Medicine, 65 Tsurumai, Showa-ku, Nagoya 466-8550, Japan. Fax: +81 52 744 2275.
E-mail address: numa2@med.nagoya-u.ac.jp (Y. Numaguchi).
[1] Present affiliation: Department of Oral Maxillofacial Prosthodontics, Kagoshima University Graduate School of Medical and Dental Sciences, Kagoshima, Japan.

http://dx.doi.org/10.1016/j.bbrc.2014.12.071
0006-291X/

alterations in IRAP knockout ($IRAP^{-/-}$) mice and to evaluate the roles of IRAP other than AngII-AT1R axis in metabolism.

2. Material and methods

All animal studies were performed in accordance with the Guide for the Care and Use of Laboratory Animals published by the US National Institute of Health. $IRAP^{-/-}$ mice were bred at the Institute for Laboratory Animal Research, Nagoya University. The derivation of $IRAP^{-/-}$ mice has been described in detail elsewhere [10,11]. The mice were derived from a 129/C57BL/6 background, and backcrossed with a C57BL/6 strain more than 12 times. C57BL/6 mice were used as wild-type (WT) controls (Chubu Kagaku Shizai, Japan). Animal experiments were performed with the authorization of the institutional review board of the Animal Care and Use Committee of Nagoya University Graduate School of Medicine. This animal study conformed to the "Position of the American Heart Association on Research Animal Use" (Circulation 1985; 71:849A). All experiments were performed using 8-week-old male mice, unless otherwise indicated.

2.1. Adipocyte cell culture

Preadipocytes were isolated from inguinal fat pads of mice as described previously [12]. Under general anesthesia with pentobarbital sodium (50 mg/kg, *i.p.*), mice adipocytes were isolated from inguinal fat pads (0.1–0.2 g) obtained from each group of mice. Adipose tissues were minced and digested with 2 mg/mL type I collagenase (Wako, Osaka, Japan) at 37 °C for 45 min. After filtration through a 100-μm filter (BD Falcon, Bedford, MA, USA) to remove cellular debris, the samples were centrifuged at 800×*g* for 5 min. Preadipocytes were then suspended in Dulbecco's modified Eagle's medium supplemented with 10% fetal bovine serum and antibiotics (100 U/mL penicillin G and 100 μg/mL streptomycin) and cultured at 37 °C, 5% CO_2. When the adherent cells had reached confluence, the attached preadipocytes were reseeded in the same medium at a concentration of 2.0×10^3 cells/cm^2. For most experiments, 1st and 2nd passage preadipocytes were used.

To induce differentiation into adipocytes, the preadipocytes were cultured in an adipogenic differentiation medium comprised of 0.5 mM 3-isobutyl-1-methylxanthine, 1 μM dexamethasone, 50 μM indomethacin, and 10 μg/mL insulin in α-MEM. After 2 weeks of differentiation, adipocytes were identified by the presence of lipid vesicles stained with Oil Red O. During the differentiation period, aliquots of conditioned medium were removed for the determination of PAI-1 antigen concentration (R&D Systems, Minneapolis, MN, USA). Adipocyte morphology during differentiation was documented under an epifluoromicroscope (BZ-8000; Keyence, Osaka, Japan) [11,13], and processed through ImageJ Version 1.37 software (BioArts, Co., Ltd., Tokyo, Japan). For quantification of triglyceride concentration in adipocytes, cells at day 14 were washed with phosphate-buffered saline twice, lysed with 0.1 M Tris–HCl, and measured using an Adipogenesis Assay Kit (Biovision, Inc., Milpitas, CA, USA).

For the analyses of metabolism, we divided 8 week-old $IRAP^{-/-}$ mice and controls (n = 12–15 each) into 4 groups in conjunction with chow types: (1) normal diet group fed a standard chow (CE-2, CLEA, JAPAN); and (2) high-fat diet group fed a high fat chow (32% fat; HFD-32, CLEA) from 8 week old for 12 weeks. During an observation period, body weight was measured every week and blood glucose was measured after 16 h deprivation of food.

2.2. Measurement of mRNA expression level

Total RNA was extracted from cell lysates or tissues using TRIzol Reagent (Invitrogen, Carlsbad, CA, USA) and the amount was quantified by a densitometer [11,13]. The first cDNA strand was synthesized using the SuperScript™ First-Strand Synthesis System (Invitrogen). Quantitative real-time PCR was performed using the LightCycler™ System (Roche Diagnostics, Mannheim, Germany) and QuantiTect™ SYBR Green PCR kit (Qiagen). Primers used were as follows: uncoupling protein-1 (UCP-1): sense, 5′-GGGCCCT TGTAAACAACAAA-3′, antisense, 5′-GTCGGTCCTTCCTTGGTGTA-3′, UCP-2: sense, 5′-GCCACTTCACTTCTGCCTTC-3′, antisense, 5′-GAAG GCATGAACCCCTTGTA-3′, UCP-3: sense, 5′-GTCTGCCTCATCAGGG TGTT-3′, antisense, 5′-CCTGGTCCTTACCATGCAGT-3′, Peroxisome proliferator-activated receptor gamma 1α (PGC-1α): sense, 5′-CC GAGAATTCATGGAGCAAT-3′, antisense, 5′-GTGTGAGGAGGGTCATC GTT-3′, Peroxisome proliferator-activated receptor-δ (PPARδ): sense, 5′-TAGAAGCCATCCAGGACACC-3′, antisense, 5′-CCGTCTTCT TTAGCCACTGC-3′, β-actin: sense, 5′-CATCCGTAAAGACCTCTATGC CAAC-3′, antisense, 5′-ATGGAGCCACCGATCCACA-3′.

2.3. Immunoblotting analysis

After 2 weeks of differentiation, adipocytes were lysed in Laemmli Sample Buffer (Sigma, St Louis, MO), and the cell lysate was used for immunoblotting analysis, as previously described [13]. The following antibodies were used in this study: rabbit anti-IRAP (sc-135229, Santa Cruz Biotechnology Inc., Santa Cruz, CA, USA), and rabbit anti-PAI-1 (AF3828, R&D Systems).

2.4. Physiological measurement

Systolic blood pressure and heart rate of mice (n = 12, each) were determined by the tail-cuff detection system Softron BP-98A (Softron, Tokyo, Japan) [11] Rectal temperature was monitored (n = 12 each) using an electronic thermometer (Model TD-300, SHIBAURA ELECTRONICS; JAPAN) equipped with a rectal probe.

Oxygen consumption (VO_2) was determined (n = 8 each) with an O_2/CO_2 metabolic measuring system (Model MK-5000, Muromachi-kikai; JAPAN). Mice were kept unrestrained in the chamber for 24 h without food. We determined VO_2 when the minimum plateau shape was obtained during light cycle, which corresponded to the period of sleep or inactivity. VO_2 is expressed as the volume of O_2 consumed per kilogram weight of lean body mass per minute [13].

2.5. Oral glucose tolerance test (OGTT) and insulin tolerance test (ITT)

OGTT and ITT were performed in each mice group after 16 h deprivation of food. Blood glucose was measured by a glucose oxidase method (NIPRO, JAPAN) at 0 min before and 20, 40, 60, and 90 min after oral glucose administration (1 mg/g body weight) via a cannula (1 mm in diameter, Natsume, Japan). Insulin was injected subcutaneously (0.7 U/kg body weight) and blood glucose was measured at 0 min before and 30, 60, 90 min after injection.

2.6. Hematological analyses

The mice (n = 8–10, each) were anesthetized by sodium pentobarbital (Dainippon Pharmaceutical, Tokyo, Japan, 33 mg/kg IP) and blood was drawn with 21G needles by the ventricle puncture method via the subxiphoid approach. Differential blood counts were obtained using an automated biochemical analyzer. Samples of mouse plasma were stored at −80 °C before measurement [11]. Plasma adiponectin and leptin concentrations were measured by sandwich enzyme-linked immunosorbent assay (Otsuka Pharmaceutical, Tokyo, Japan). [4,5] Active PAI-1 levels were measured with an ELISA kit using the binding of PAI-1 to mouse recombinant

u-PA (murine PAI activity assay kit, Innovative Research Inc., Southfield, MI, USA) [11].

2.7. Adipose tissue morphometric analysis

The epididymal fat pad for WAT and intrascapular area for BAT were removed and stained by hematoxylin and eosin (H&E) followed by morphometric analyses [11].

2.8. CT scan analysis

The adiposity of mice was examined radiographically using CT (La Theta, ALOKA, JAPAN) according to the manufacture's protocol. We performed CT scanning at 2-mm intervals from the diaphragm to the bottom of the abdominal cavity [13].

2.9. Statistical analysis

The data are presented as means ± SEM values, unless otherwise indicated. Statistical analysis of multiple comparisons among the groups was conducted by one-way ANOVA followed by the Bonferroni test. Statistical analysis of comparisons between two groups over time used repeated measures ANOVA. Multiple comparisons in nonparametric analysis were performed by the Kruskal–Wallis test. A probability value of $P < 0.05$ was considered significant.

3. Results

3.1. Decrease of adipocyte lipid droplet size in $IRAP^{-/-}$ mice

At first, to evaluate the morphological and functional differences of adipocytes between wild-type (WT) and $IRAP^{-/-}$ mice, we observed the process of adipocyte differentiation prepared from epididymal fat pads of each group of mice. In the cell culture of adipocytes, image analysis indicated that the size of lipid droplets within the cells was decreased after incubation for 14 days (Fig. 1A). In addition, the number of cells containing lipid droplets was also decreased as revealed by Oil Red O staining (39.5 ± 4.5 vs. 24.3 ± 2.3 cells/mm^2, respectively; $P < 0.01$). The average triglyceride concentration was significantly lower in cells from $IRAP^{-/-}$ mice than from WT mice (16.2 ± 3.1 vs. 32.3 ± 8.2 nmol/L, respectively; $P < 0.01$).

3.2. Induction of IRAP and reduced PAI-1 production during adipocyte differentiation

During the process of differentiation from preadipocytes to mature adipocytes, we observed upregulation of IRAP protein in the culture cells from WT mice. The expression levels increased by 2.4-fold at 14 days after incubation ($P < 0.01$, Supplemental Fig. IA).

Previously, we demonstrated that PAI-1 induction in response to angiotensin II (AngII) was diminished in cultured endothelial cells from $IRAP^{-/-}$ mice compared to WT mice [11]. PAI-1 is a key regulator and potential marker of adipocyte differentiation as well as fibrinolysis. We measured PAI-1 gene and protein expression levels at 2 and 14 days after incubation, and PAI-1 antigen levels in the medium were measured during adipocyte differentiation over 10 days. PAI-1 mRNA and protein levels were lower at day 14 in the medium from $IRAP^{-/-}$ mice ($P < 0.05$, Fig. 1B and C). PAI-1 secretion levels from adipocytes from $IRAP^{-/-}$ mice were concomitantly lower than those of WT mice ($P < 0.05$, Supplemental Fig. IB), suggesting lower induction levels of PAI-1 during adipocyte differentiation in $IRAP^{-/-}$ mice, as similarly observed in endothelial cells.

3.3. Basal characteristics of $IRAP^{-/-}$ mice

The basal characteristics of $IRAP^{-/-}$ mice are shown in Supplemental file Table I. Body weight, fat weight evaluated by the ratio of epididymal fat weight to body weight, and heart rate, were similar between groups. With respect to glucose and lipid metabolism, $IRAP^{-/-}$ mice showed no differences in the basal levels of glucose, insulin, cholesterol, triglycerides or free fatty acids, compared with WT mice [11].

3.4. $IRAP^{-/-}$ mice are protected from diet-induced obesity

On a standard diet, body weight gain was comparable between WT and $IRAP^{-/-}$ mice during an observation period (26.4 ± 0.61 vs. 25.4 ± 0.72 g; P = NS). We, next, examined the effect of a high-fat diet on the metabolic phenotypes of $IRAP^{-/-}$ mice [13]. WT mice fed a high-fat diet weighed 45% more than those fed a normal chow (40.2 ± 1.2 vs. 26.4 ± 0.61 g; $P = 0.008$). After 12 week, the average body weight of $IRAP^{-/-}$ mice was 30.5 ± 2.7 g, which was 25% lower than that of WT mice fed a high-fat diet (Fig. 2). Reduced adiposity of $IRAP^{-/-}$ mice fed a high-fat diet was confirmed in the ratio of epididymal fat weight to body weight (0.028 ± 0.002 vs. 0.041 ± 0.004; $P < 0.01$) and CT scanning (Fig. 2C). The average of abdominal fat content analyzed by CT scanning was significantly lower in $IRAP^{-/-}$ mice (5.21 ± 0.82% vs. 15.3 ± 4.4% for WT, $P = 0.006$). Sections of white adipose tissue (WAT) from $IRAP^{-/-}$ mice showed decreased adipocyte size relative to controls and the average area of adipocytes was smaller in $IRAP^{-/-}$ mice than that of WT mice (2560 ± 160 vs. 4120 ± 330 μm^2, $P < 0.001$, Fig. 2D and Supplemental Fig. IC). In the sections of brown adipose tissue (BAT), lipid accumulation after a high-fat diet was decreased in $IRAP^{-/-}$ mice compared with WT mice (Fig. 2E).

3.5. Alterations in metabolic parameters in $IRAP^{-/-}$ mice

To assess metabolic causes of the resistance of $IRAP^{-/-}$ mice against food-induced obesity, we compared saccharometabolism, rectal temperature, food intake, and basal metabolic rate between $IRAP^{-/-}$ and WT mice fed a high-fat diet. Regarding lipid metabolism, significant decreases were observed in serum cholesterol concentrations in $IRAP^{-/-}$ mice after a high-fat diet, whereas there were no significant differences in serum triglyceride and free fatty acid between groups before and after a high-fat diet (Supplemental Table II). Oral glucose test and insulin tolerance test revealed that the glucose disposal and the hypoglycemic effect of insulin did not differ between groups before a high-fat diet, but both of those were pronounced in $IRAP^{-/-}$ mice after a high-fat diet (Supplemental Fig. II). These results suggest that $IRAP^{-/-}$ mice maintained better glucose tolerance and insulin sensitivity after a high fat diet challenge. In relation to obesity and secretion of adipocytokines [14], the high-fat diet decreased plasma adiponectin levels in either group with a greater degree in WT mice if compared with in $IRAP^{-/-}$ mice ($P < 0.05$). Similarly, plasma leptin levels increased with a greater degree in WT mice ($P < 0.05$) (Supplemental Fig. IIE and IIF).

Since an excess of body weight results from an imbalance between food intake and energy expenditure [13–17], we compared the locomotor activity and basal metabolic rates using an indirect calorimeter [13]. Although no difference was observed in daily food intake and physical activity between groups (Fig. 3A and B, Supplemental Tables), $IRAP^{-/-}$ mice revealed mild hyperthermia by 0.42 ± 0.05 °C in rectal temperature (37.8 ± 0.21 vs. 38.2 ± 0.25 °C, $P = 0.026$) and increased whole-body oxygen consumption rates (45.9 ± 0.70 vs. 57.4 ± 0.71 ml/kg/min, $P = 0.0056$) relative to WT mice (Fig. 3C and D).

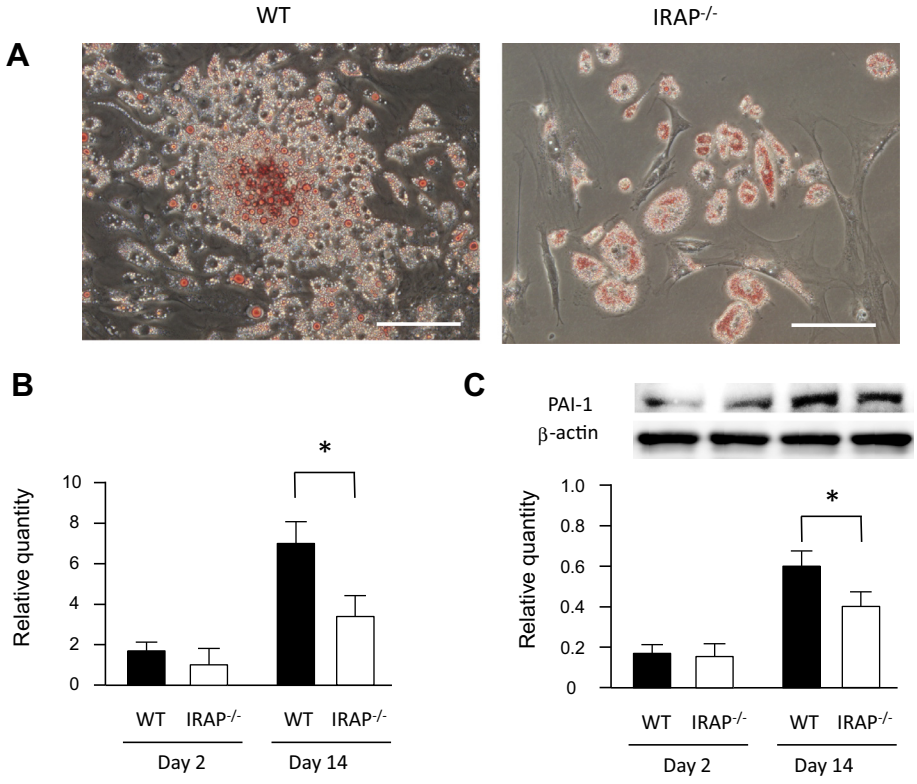

Fig. 1. Adipocyte differentiation and lipid droplet formation. (A) Representative photomicrographs of adipocytes. Lipid droplets were stained with Oil Red O. Bars, 50 μm. (B and C) PAI-1 gene (B) and protein (C) expressions in adipocytes at days 2 and 14 after incubation. (C) The levels of PAI-1 gene were suppressed in adipocytes from IRAP$^{-/-}$ mice after 14 day incubation. $^{*}P < 0.05$. (C) The upper lane depicts IRAP and the lower β-actin protein expressions, respectively. Similar to PAI-1 gene expression pattern, the levels of PAI-1 protein were suppressed IRAP$^{-/-}$ mice after 14 day incubation. $^{*}P < 0.05$. The results are expressed as the mean ± standard deviation (SD).

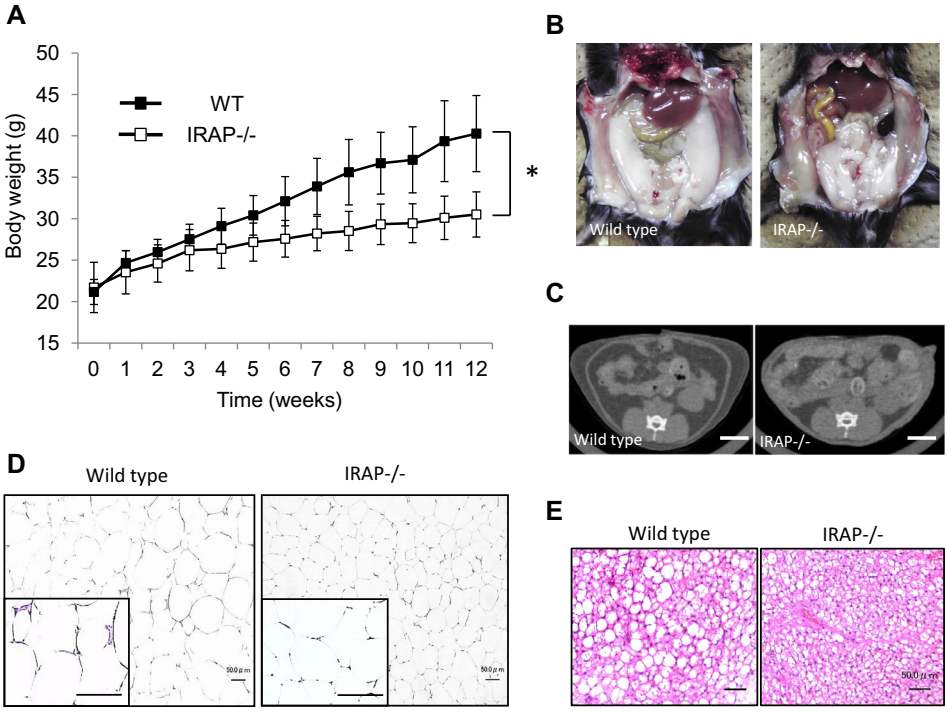

Fig. 2. Protection from diet-induced obesity in IRAP$^{-/-}$ mice. (A through E), Body weight gain and adiposity were suppressed in IRAP$^{-/-}$ mice. (A) Time course of body weight changes. Mice were given a high fat diet at age of 8 weeks for 12 weeks. $^{*}P < 0.05$. (B) Gross sections. Note that the volume of epididymal fat in IRAP$^{-/-}$ mice was smaller than that of WT mice. (C) CT scanning at the navel level. Bars are 5 mm. (D) Histological analysis of WAT. Note that, in WT mice, clustering of macrophages is observed frequently around adipose tissue. Bars are 50 μm. (E) Sections from BAT. Bars are 50 μm. Results are expressed as mean ± SD.

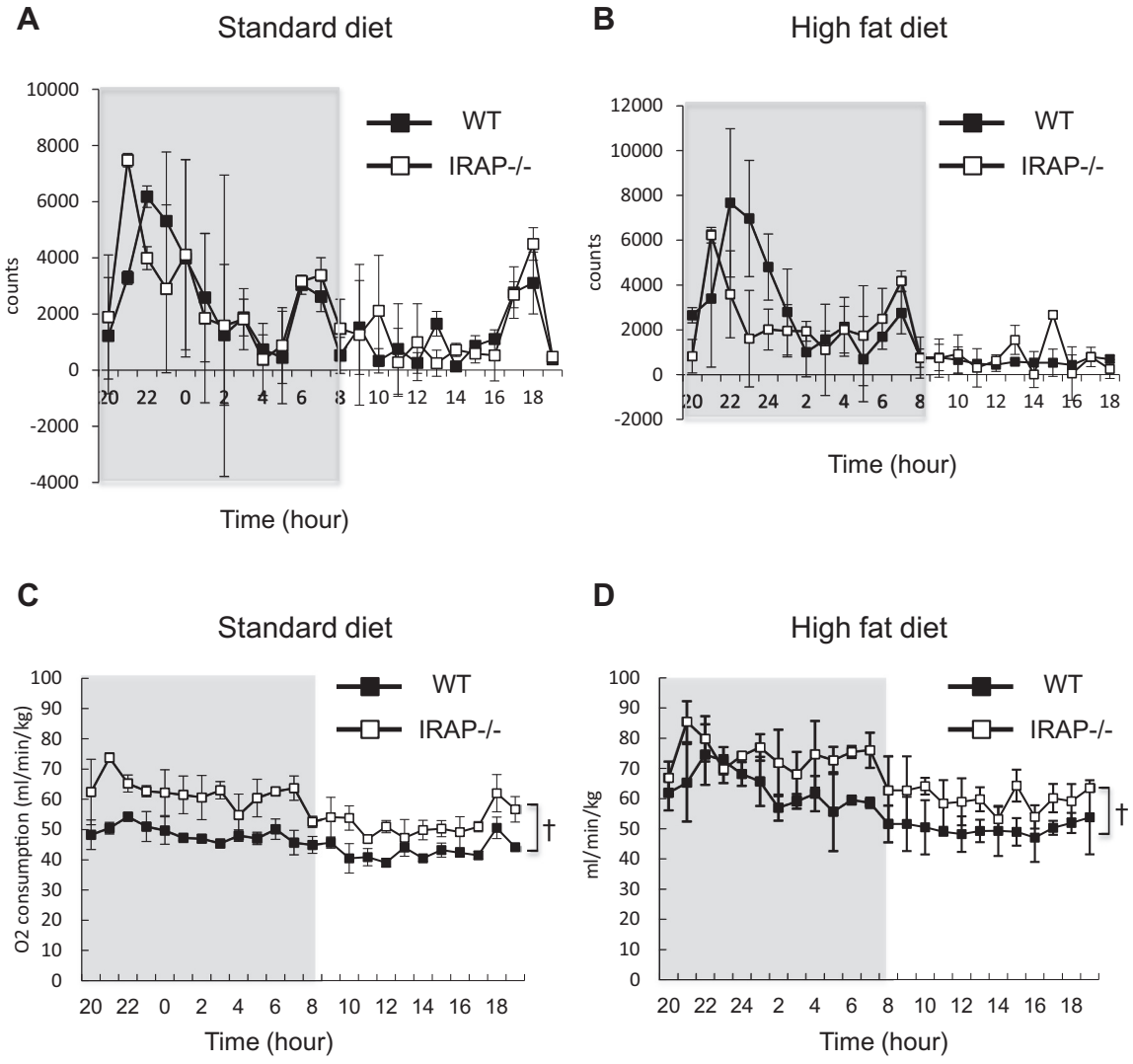

Fig. 3. Physical activity and metabolic rates. (A and B) Physical activity on a standard diet (A), and on a high fat diet (B). (C and D) Oxygen consumption on a standard diet (C) and on a high fat diet (D). Although significant difference was not observed in physiological activity, oxygen consumption rate was higher in IRAP$^{-/-}$ mice than in WT mice before and after a high fat loading. $^{\dagger}P < 0.01$. Gray shadow depicts dark time.

3.6. Increased energy expenditure in BAT in IRAP$^{-/-}$ mice

We investigated the molecular alterations focusing on energy metabolisms in skeletal muscles and BAT [14–16]. In soleus and gastrocnemius muscle that are characterized with red fiber- and white fiber-dominant muscle, respectively, there were no differences in uncoupling protein (UCP)-2, UCP-3, peroxisome proliferator-activated receptor-γ coactivator (PGC)-1α and peroxisome proliferator-activated receptor (PPAR)-δ, which predominantly regulate thermogenesis in muscle. (Supplemental Fig. III) In contrast, the levels of UCP-1, which is a key regulator of thermogenesis in adipose tissue, were 4.0-fold higher in BAT from *IRAP*$^{-/-}$ mice if compared with those of WT mice after a high-fat diet (Fig. 4A–C). Further, Regarding adaptation to cold, UCP-1 levels in BAT were elevated to a similar level of WT mice observed at room temperature, suggesting that adaptive thermogenesis was not impaired in *IRAP*$^{-/-}$ mice (Fig. 4D).

4. Discussion

We have investigated a critical role of the IRAP in obesity and energy metabolism by comparing *IRAP*$^{-/-}$ mice with WT controls. *IRAP*$^{-/-}$ mice fed a standard chow exhibited comparable body weight gain and adiposity to WT mice, whereas, after a high fat diet, body weight gain and obesity were significantly suppressed in *IRAP*$^{-/-}$ mice with increased energy expenditure via upregulation of UCP-1 in BAT.

Regarding RAS activity and obesity, accumulating evidence from clinical studies indicates that RAS blockade leads to body weight loss with the improvement of insulin sensitivity [1–6]. Downstream of the AngII-AT1R cascade, AngIV, which is derived by the cleavage of 2 N-terminal amino acids by aminopeptidases, binds to its receptor, IRAP, and activates many intracellular signaling pathways such as PAI-1 [10,11,18,19]. PAI-1 induction is evoked through IRAP activation in endothelial cells independent to the AngII-AT1R axis [5,6,20]. Previously, we demonstrated that PAI-1 induction is impaired in endothelial cells from *IRAP*$^{-/-}$ mice after AngII and AngIV treatment [11]. In the present study, during the differentiation of preadipocytes to adipocytes, active PAI-1 levels were consistently lower in cultured cells from *IRAP*$^{-/-}$ mice than from WT mice (Fig. 2E). Morphometrical analysis revealed that the differentiation of preadipocytes to adipocytes and lipid accumulation within adipocytes were significantly suppressed (Fig. 1A–C). This multilocular morphology with smaller lipid

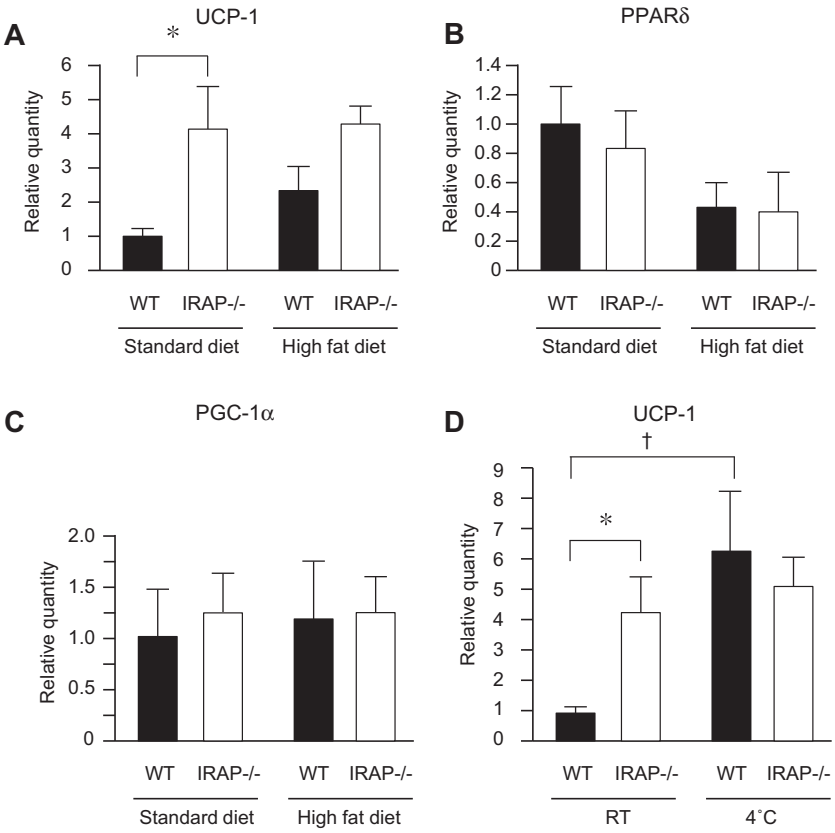

Fig. 4. Upregulation of UCP-1 levels in BAT at basal and cold conditions. (A–C) Thermogenesis-associated genes expression in BAT. (D) Upregulation of UCP-1 levels in IRAP$^{-/-}$ mice. In WT, UCP-1 levels increase after adaptation to cold, whereas, in IRAP$^{-/-}$ mice, the levels were upregulated before cold adaptation. The part of UCP-1 levels at room temperature is same as figure A. RT depicts room temperature. $^{*}P < 0.05$ and $^{\dagger}P < 0.01$.

droplets observed in the adipocytes of *IRAP*$^{-/-}$ mice, with a higher surface to volume ratio, will facilitate the release of their stored lipids and may lead to the greater degree of glucose uptake and higher insulin sensitivity in *IRAP*$^{-/-}$ mice [21]. Concomitantly, *in vivo*, lipid accumulation in WAT and BAT was decreased with lower active PAI-1 levels and a higher ratio of plasma adiponectin to PAI-1 after a high-fat diet was given to *IRAP*$^{-/-}$ mice. These results are similar to those of PAI-1-deficient mice or mice with pharmacological intervention against PAI-1 activity that are resistant to diet-induced obesity [18,19].

In downstream of AngII-AT1R cascade, AngIV binds its receptor, IRAP, and activates many intracellular signaling pathways [7–11,17,20]. In our study, *IRAP*$^{-/-}$ mice were protected from diet-induced body weight gain and obesity through the increased energy expenditure with mild hyperthermia, which did not seem to be due to altered food intake, locomotor activity, sympathetic activity, or thyroid hormones but was strongly associated with upregulation of UCP-1 in BAT. Originally BAT was thought to function in newborn babies in resistance to cold [14–16,21–23]. However, recent accumulating data have demonstrated that adult humans also have functional BAT and that pharmacological enhancement of BAT function would be an alternative strategy against obesity other than calorie restriction and increase of physical activity [21–23]. In this regard, further investigations to clarify the relation between IRAP/AT4R blockade and UCP-1 upregulation may provide a cue to solve the issue of BAT activation in adults and produce a novel drug against obesity without modifying the appetite or behavior.

In conclusion, IRAP deficiency may lead to suppression of PAI-1 expression in the development of adipocytes and upregulation of UCP-1-mediated thermogenesis in BAT and increased energy expenditure to prevent the development of obesity. Intervention of IRAP may be a potential strategy against obesity and subsequent metabolic syndrome, diabetes, and cardiovascular diseases.

Funding sources

None.

Disclosures

None.

Acknowledgments

The animal study was performed at the Institute for Laboratory Animal Research, Nagoya University and Department of Molecular Genetics, Kumamoto University.

Appendix A. Supplementary data

Supplementary data associated with this article can be found, in the online version, at http://dx.doi.org/10.1016/j.bbrc.2014.12.071.

References

[1] A. Prasad, A.A. Quyyumi, Renin–angiotensin system and angiotensin receptor blockers in the metabolic syndrome, Circulation 110 (11) (2004) 1507–1512.
[2] R.E. Schmieder, K.F. Hilgers, M.P. Schlaich, B.M. Schmidt, Renin–angiotensin system and cardiovascular risk, Lancet 369 (2007) 1208–1219.
[3] S. Thatcher, F. Yiannikouris, M. Gupte, L. Cassis, The adipose renin–angiotensin system: role in cardiovascular disease, Mol. Cell. Endocrinol. 302 (2) (2009) 111–117.

[4] P.B. Timmermans, P.C. Wong, A.T. Chiu, W.F. Herblin, P. Benfield, D.J. Carini, R.J. Lee, R.R. Wexler, J.A. Saye, R.D. Smith, Angiotensin II receptors and angiotensin II receptor antagonists, Pharmacol. Rev. 45 (1993) 205–251.
[5] R. Kouyama, T. Suganami, J. Nishida, M. Tanaka, T. Toyoda, M. Kiso, T. Chiwata, Y. Miyamoto, Y. Yoshimasa, A. Fukamizu, M. Horiuchi, Y. Hirata, Y. Ogawa, Attenuation of diet-induced weight gain and adiposity through increased energy expenditure in mice lacking angiotensin II type 1a receptor, Endocrinology 146 (8) (2005) 3481–3489.
[6] R. Yamamoto, H. Akazawa, H. Fujihara, Y. Ozasa, N. Yasuda, K. Ito, Y. Kudo, Y. Qin, Y. Ueta, I. Komuro, Angiotensin II type 1 receptor signaling regulates feeding behavior through anorexigenic corticotropin-releasing hormone in hypothalamus, J. Biol. Chem. 286 (24) (2011) 21458–21465.
[7] A.L. Albiston, S.G. McDowall, D. Matsacos, P. Sim, E. Clune, T. Mustafa, J. Lee, F.A. Mendelsohn, R.J. Simpson, L.M. Connolly, S.Y. Chai, Evidence that the angiotensin IV (AT(4)) receptor is the enzyme insulin-regulated aminopeptidase, J. Biol. Chem. 276 (52) (2001) 48623–48626.
[8] S.R. Keller, H.M. Scott, C.C. Mastick, R. Aebersold, G.E. Lienhard, Cloning and characterization of a novel insulin-regulated membrane aminopeptidase from Glut4 vesicles, J. Biol. Chem. 270 (40) (1995) 23612–23618.
[9] I. Jordens, D. Molle, W. Xiong, S.R. Keller, T.E. McGraw, Insulin-regulated aminopeptidase is a key regulator of GLUT4 trafficking by controlling the sorting of GLUT4 from endosomes to specialized insulin-regulated vesicles, Mol. Biol. Cell 21 (12) (2010) 2034–2044.
[10] S.R. Keller, A.C. Davis, K.B. Clairmont, Mice deficient in the insulin-regulated membrane aminopeptidase show substantial decreases in glucose transporter GLUT4 levels but maintain normal glucose homeostasis, J. Biol. Chem. 277 (20) (2002) 17677–17686.
[11] Y. Numaguchi, M. Ishii, R. Kubota, Y. Morita, K. Yamamoto, T. Matsushita, K. Okumura, T. Murohara, Ablation of angiotensin IV receptor attenuates hypofibrinolysis via PAI-1 downregulation and reduces occlusive arterial thrombosis, Arterioscler. Thromb. Vasc. Biol. 29 (12) (2009) 2102–2108.
[12] P. Björntorp, M. Karlsson, P. Pettersson, G. Sypniewska, Differentiation and function of rat adipocyte precursor cells in primary culture, J. Lipid Res. 21 (1980) 714–723.
[13] Y. Oike, M. Akao, K. Yasunaga, T. Yamauchi, T. Morisada, Y. Ito, T. Urano, Y. Kimura, Y. Kubota, H. Maekawa, T. Miyamoto, K. Miyata, S. Matsumoto, J. Sakai, N. Nakagata, M. Takeya, H. Koseki, Y. Ogawa, T. Kadowaki, T. Suda, Angiopoietin-related growth factor antagonizes obesity and insulin resistance, Nat. Med. 11 (4) (2005) 400–408.
[14] H. Katagiri, T. Yamada, Y. Oka, Adiposity and cardiovascular disorders: disturbance of the regulatory system consisting of humoral and neuronal signals, Circ. Res. 101 (1) (2007) 27–39.
[15] Y.H. Tseng, A.M. Cypess, C.R. Kahn, Cellular bioenergetics as a target for obesity therapy, Nat. Rev. Drug Discov. 9 (6) (2010) 465–482.
[16] B.M. Spiegelman, J.S. Flier, Obesity and the regulation of energy balance, Cell 104 (4) (2001) 531–543.
[17] L.P. Kozak, M.E. Harper, Mitochondrial uncoupling proteins in energy expenditure, Annu. Rev. Nutr. 20 (2000) 339–363.
[18] M.C. Alessi, I. Juhan-Vague, PAI-1 and the metabolic syndrome: links, causes, and consequences, Arterioscler. Thromb. Vasc. Biol. 26 (2006) 2200–2207.
[19] B.M. De Taeye, T. Novitskaya, L. Gleaves, J.W. Covington, D.E. Vaughan, Bone marrow plasminogen activator inhibitor-1 influences the development of obesity, J. Biol. Chem. 281 (2006) 32796–32805.
[20] V. Esteban, M. Ruperez, E. Sánchez-López, J. Rodríguez-Vita, O. Lorenzo, H. Demaegdt, P. Vanderheyden, J. Egido, M. Ruiz-Ortega, Angiotensin IV activates the nuclear transcription factor-kappaB and related proinflammatory genes in vascular smooth muscle cells, Circ. Res. 96 (9) (2005) 965–973.
[21] D. Barneda, A. Frontini, S. Cinti, M. Christian, Dynamic changes in lipid droplet-associated proteins in the "browning" of white adipose tissues, Biochim. Biophys. Acta 1831 (2013) 924–933.
[22] A.M. Cypess, S. Lehman, G. Williams, I. Tal, D. Rodman, A.B. Goldfine, F.C. Kuo, E.L. Palmer, Y.H. Tseng, A. Doria, G.M. Kolodny, C.R. Kahn, Identification and importance of brown adipose tissue in adult humans, N. Engl. J. Med. 360 (15) (2009) 1509–1517.
[23] K.A. Virtanen, M.E. Lidell, J. Orava, M. Heglind, R. Westergren, T. Niemi, M. Taittonen, J. Laine, N.J. Savisto, S. Enerbäck, P. Nuutila, Functional brown adipose tissue in healthy adults, N. Engl. J. Med. 360 (15) (2009) 1518–1525.